An Open-Source Passively Sprawling Miniature Legged Robot

Adam Stager*, Konstantinos Karydis*, and Herbert G. Tanner

***Abstract*— The paper reports on the design and preliminary experimental testing of a novel 3D-printed miniature legged robot. It is called Passively Sprawling Robot (PSR), and it features a mechanism that achieves passive adjustment of the sprawl angle of the robot's legs. Passive sprawling in this robot exhibits compliance by design, yet it can be controlled indirectly by regulating the yaw rate. Spring-loaded leg assemblies on the left and right side of the robot rotate independently, allowing the vehicle to overcome asymmetrical obstacles with improved lateral stability, and withstand falls from moderate heights without sustaining structural damage. The regulation of the sprawling angle by means of varying yaw rates, as well as the improved motion characteristics have been experimentally observed and verified, and open-loop motion accuracy along straight and constant curvature paths was tested on a number of repeated trials.**

I. Introduction

Advances in novel fabrication processes have enabled the development of a variety of miniature legged robots. Examples include the underactuated robots i-Sprawl [1], Mini-Whegs [2], [3] and STAR [4], as well as the direct-drive robot [5]. The Smart Composite Microstructure (SCM) technique [6] has contributed to the development of minimally actuated palm-sized crawling robots, including DynaRoACH [7], OctoRoACH [8] and VelociRoACH [9].

Miniature legged robots show promise in enhancing our technical capabilities in application areas like search-and-rescue and intelligence–surveillance–reconnaissance (ISR). Interesting features are brought to bare that create new opportunities for mobility in challenging environments involving tight and confined spaces. In addition, rapid and cost-effective production facilitates deployment in larger numbers.

Achieving all-terrain mobility, however, is challenging [10]. In particular, adapting to terrain variations is key to take the robots outside of the protected laboratory environment, and deploy them in real-world settings. In an effort to meet this challenge, compliance in robot design has been deliberately introduced: for instance, the legged platform RHex [11] incorporates compliant legs to successfully traverse a variety of terrains; SeaDog [12] features torsionally compliant wheel-legs for shock absorption and support while climbing over obstacles; SprawlHex [13] can adjust its body sprawl angle to achieve insect-like behaviors. These design paradigms have been mirrored in the miniature scale: Robots of the RoACH family [7]–[9] use compliant linkages to drive their legs—also compliant—and STAR [4] actively regulates its sprawl angle to crawl beneath, or climb over obstacles.

This work is supported by ARL MAST CTA # W911NF-08-2-0004.

Adam Stager, Konstantinos Karydis, and Herbert Tanner are with the Department of Mechanical Engineering, University of Delaware.
Email: {astager, kkaryd, btanner}@udel.edu
* These authors contributed equally to this work

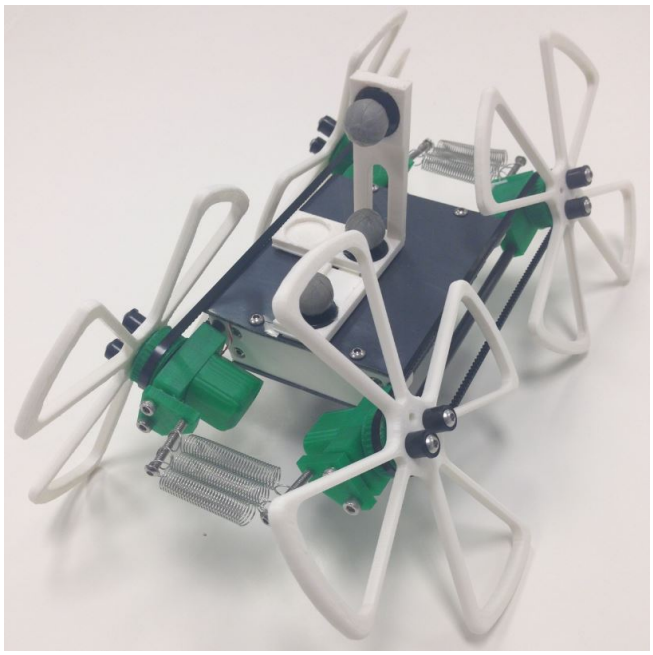

Fig. 1. The 3D-printed Passively Sprawling Robot (PSR). Its main body is 18 cm-long and 11 cm-wide. The robot features twso side pivots which support a wheel-leg design, and a passive spawl-adjusting mechanism to adapt to terrain variations.

Drawing motivation from the active sprawl-adjusting mechanism of STAR and the torsionally compliant legs of SeaDog, this paper reports on the design of a new 3D-printed miniature legged robot. The robot is called Passively Sprawling Robot (PSR), and features a *passive* sprawl-adjusting mechanism (Fig. 1). It is a light-weight (< 350 g), low-cost (< 150 USD) robot that can be manufactured without the need for expensive, specialized equipment. The components of the main body and side pivots, as well as the driving electronics can all be put together using off-the-shelf parts.

PSR is able to passively adjust its sprawl angle to negotiate uneven terrain. In fact, its two sides can passively achieve different sprawling angles in order for the robot to traverse terrain with high variability. Transitioning between upward and downward sprawl configurations is achieved through body rotations at different yaw rates. Preliminary experimental testing suggests that passive compliance promotes lateral stability when the robot overcomes asymmetrical obstacles.

The work reported in this paper contributes to achieving all-terrain mobility capabilities with miniature legged robots at low cost. Since power autonomy is an important oper-

ational factor in this realm, integrating passive compliance mechanisms within the robot is advantageous from the point of view of weight and need for actuation, without compromizing mobility and the ability to negotiate obstacles or traverse uneven terrain. In fact, as experimental evidence in this paper suggests, the type of passive compliance introduced, increases robustness and impact survivability.

II. Design Characteristics

A. Design and manufacturing

The entire frame of the robot is 3D-printed using a Makerbot Replicator 2. Individual parts are bolted together, allowing for easy assembly and quick part replacement in case of damage. The main body of the robot consists of a water-safe case that houses all electronics (Arduino Fio, XBee, motor driver, and step-up voltage regulator) and two 3.7V Li-Po batteries, and springs that connect the two pivot sides of the robot (Fig. 3). PSR features two Pololu micro 298:1 gearmotors, each driving all legs of a single side. Printing all parts for the robot takes about 4 hrs under standard quality printer settings; assembly is fast and requires only basic hardware and soldering skills. The total assembled weight of the robot is measured at 334g.

A significant design modification compared to STAR is the transition from six to four legs. It is difficult to reliably produce gears of this size with moderately-priced 3D printers, and transmissions consisting of such gears suffer from severe backlash. On the other hand, a timing belt and pulley system eliminates most of the additional shear stresses that cause failure of the gear teeth, and allows for smooth rotation of the drive components and legs. To minimize the complexity of the transmission mechanism, a simple two-pulley design is used (Fig. 2), thus reducing the total number of legs from six to four. A 90^o spacing between the rounded spokes of each leg ensure quasi-static stability.

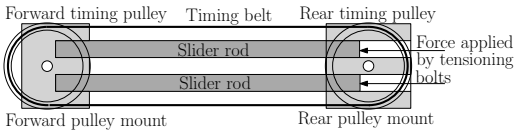

Fig. 2. Two sliding rods make up a frame for each pivot side of the robot. The timing belt is tensioned with two screws that apply pressure to the sliding rods. The tensioned timing belt then holds the front and rear pulley mounts together.

The robot features rounded spoke legs (Fig. 1). Rounded spokes have been observed to behave increasingly more like their wheel counterparts as the sprawl angle increases [4]. In the design depicted in Fig. 3, the planes on which the wheel legs lay can passively rotate in the roll direction relative to the robot's body, allowing the platform to sprawl. In general, increasing the sprawl angle can result in improved stability, as it redirects ground reaction forces inward, i.e., toward the robot body, where they partially cancel. The ability to sprawl is a design characteristic which is shared with STAR, only here the sprawling motion is not actuated, the two belt driven sides can attain different sprawl angles depending on terrain conditions, and the sprawling motion is passively compliant.

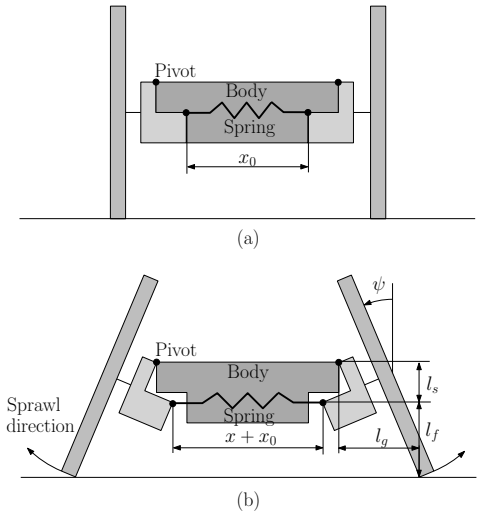

Fig. 3. (a) The upright configuration the robot has maximum ground clearance, (b) As the robot sprawls a spring produces restoring forces.

B. Passive sprawl compliance

Compliance is often seen as a challenge in robotics due to the additional degrees of freedom and possibly the introduction of non-linearity in the system dynamics. Yet, it has been documented [14], [15] that compliance can improve stability in locomotion. The design reported here involves a laterally focused compliant mechanism, which passively adjusts the overall height of the vehicle. When asymmetrically traversing obstacles from an upright posture—for example when only one side interacts physically with an obstacle—the compliant mechanism allows the side of the robot in contact with the obstacle to sprawl asymmetrically. This type of terrain traversal, where different sides interact with the ground asymmetrically, is quite common for miniature vehicles moving on irregular, uneven surfaces (e.g. pebbles or small steps). The ability to sprawl on one side has a stabilizing effect on the vehicle, by reducing the center-of-mass vertical displacement, and the longitudinal twisting that can cause inadvertent changes in straight-line motion.

The steady-state behavior of the robot under sustained running is adjusted by varying the level of spring tension. Certain missions might require a type of motion similar to that of wheeled vehicles, achieved with PSR operating at increased sprawl angles, whereas traversing rougher terrain can call for the robot maintaining a more upright posture. By increasing the spring constant we observed decreased sprawl angles. With reference to Fig. 3, let ψ express the sprawl angle, and denote M_p the moment about the sprawl pivot, $\ell_s(\psi)$ the moment arm of the spring, $\ell_g(\psi)$ and $\ell_f(\psi)$ moment arms due to the spoked legs sprawl, and g the acceleration of gravity. x_0 denotes the initial length of the spring and $x(\psi)$ its length when stretched. Then,

$$M_p = -k\ell_s(x + x_0) + m\ell_g g - f_k \ell_f mg \ . \qquad (1)$$

The moment about the sprawl pivot, M_p is calculated as the sum of moments created as the spring and frictional

forces oppose the gravitational force. A kinetic frictional force f_k acts on the spoke in contact with the ground, thus opposing the moment induced by gravity.

The angle of sprawl can also be tuned actively with the use of the existing drive motors, thus eliminating the use of an additional motor for sprawl adjustment. By spinning at higher angular velocities the increased normal force induces larger lateral friction forces on the wheel-legs. This increase in frictional force results in a gradual reduction in sprawling angle, manifested in a composite motion where the robot spins around the vertical axis and moves its center of mass up as its legs straighten vertically. This phenomenon practically gives rise to a novel mobility characteristic, where the robot spins to passively straighten its legs in order to traverse rough terrain or obstacles which may be insurmountable otherwise.

When spinning at lower angular velocities the additional friction force is no longer present so the robot slips down into a low sprawl configuration. Although the moment arm on which gravitational force acts increases as the degree of sprawl increases—see (1)—due to the placement of the spring on the pivot joint there is also an increase in spring tension. This canceling effect allows the robot to remain in the sprawled configuration and continue in a straight line, overcoming gravity and achieving an upright posture even when starting at maximum sprawl angle.

III. Description of Motion Capabilities

When the robot is in an upright configuration (Fig. 3(a)), ground reaction forces result in significant vertical perturbations which cause bouncing effects, additional energy consumption and reduce the maximum speed the robot can achieve [5]. Sprawling, on the other hand, leads to robot behaviors that are qualitatively closer to those observed in insects [13]. Additionally, studies on the motion of STAR [4], [16] show that low sprawl configurations lead to smoother and more stable motion behaviors. We anticipate that the passive sprawl adjustment will aid in cancelling such disturbances; the validity of this hypothesis is tested in Section IV.

A. Passive lateral stability

Lateral stability has been recognized as a challenge in wheeled vehicles traversing uneven terrain [3]. When an obstacle is placed in a way that would cause roll-instability, the recommended strategy is to approach the obstacle head-on in order to avoid tipping on one side. Legged robots, on the other hand, often benefit from the additional degrees of freedom offered by the multiple joints between the robot's center of mass and the supporting surface interface. Studies suggest that longitudinal flexibility may increase stability against flip-over when climbing over tall head-on obstacles [17]; however no works that directly address lateral stability in such tasks seem to be available.

PSR can traverse uneven terrain with high variability without tipping over. Its pivot sides can passively achieve asymmetrical sprawling angles, allowing the robot to self-adjust its body posture depending on the terrain, and navigate smoothly. As indicated in Fig. 4, this capability is due to the physical constraint on the low-side legs; this side is not allowed to sprawl while the legs on the obstacle are free to rotate. Thus, the side in contact with the obstacle sprawls, and the robot lowers its center of mass, improving stability.

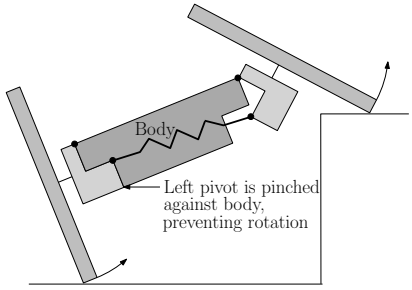

Fig. 4. The physical constraint on leg swing allows for asymmetrical sprawl when starting from the upright configuration.

B. Drop robustness

It has been documented [3] that spoked wheel-legs result in high force concentrations which can cause failure. The effect of these force concentrations becomes particularly pronounced during impact. Impact instances can be quite common for the type of robots considered, when deployed over uneven terrain; for instance, the robot might have to get down a flight of stairs, or fall from an elevated surface (rock, ceiling, etc.). Sprawl compliance, depending on the impact angle, may increase the time of impact, effectively reducing the maximum force concentrations, and thus increasing the robot's chances to endure that impact.

C. Slope traversal

In general, increased sprawl angles lower the center of mass of the robot, increasing lateral stability. Sprawling can have the same stabilizing effect when moving forward on an incline; this time, there is no relative roll rotation between the robot's components along the direction of motion, but reducing ground clearance has the same stabilizing effect on pitch motion which can cause the vehicle to flip backward. At the same time, sprawling has minimal to no effect on the magnitude of friction forces that support traction. For this reason, the test results on slope traversal reported in Section IV speak only to the ability of the vehicle to avoid flip-over when moving forward on an incline, rather than being able to cover distance in the longitudinal direction.

D. High speed crawling

The robot is capable of high-speed crawling by simply removing two bolts and swapping gearmotors. A wide range of these motors are readily available off-the-shelf, and can be chosen depending on the application. In the current setting, we used Pololu 298:1 gearmotors which result in top speeds of about 3.25 body lengths per second at 75% of their maximum voltage output (6 V).

IV. Experimental Testing

This section reviews experimental results that corroborate the predictions of Section III. The assessment is based on open-loop position and heading data collected while PSR moved on a rubber floor mat surface. When testing against obstacles, a jig was used to reduce error in initial position and ensure proper heading of the PSR with respect to obstacles.

A. Effect of sprawl on elementary motion behaviors

We consider three families of elementary behaviors: (i) straight-line motion, (ii) constant-curvature turns, and (iii) turn-in-place motion. We focus on testing two different initial sprawl configurations; $\psi_{up} = 0^o$ (upright initial configuration), and $\psi_{sp} = 50^o$ (sprawled initial configuration). Figures 5 and 6 present the evolution of the robot's center-of-mass position in straight-line and constant-curvature paths, collected using a Vicon motion capture system.

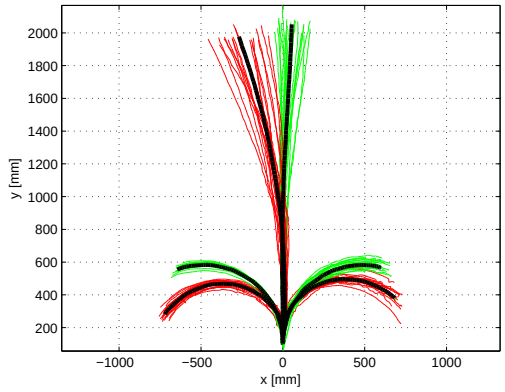

Fig. 5. Straight line, clockwise and counter-clockwise turns for PSR. Paths corresponding to upright initial configurations (in red) display substantial error when compared to those corresponding to sprawled initial configurations (in green). Experimental averages are marked in black. Notice the distinct path radii caused by different initial sprawl postures.

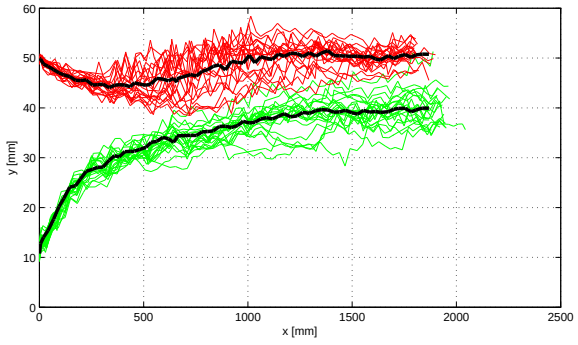

Fig. 6. The robot passively regulates its sprawl angle and appears to converge to a steady-state height when moving in straight-line paths. Paths starting at an upright initial configuration are shown in red, while paths from sprawled initial configuration are shown in green. Curves in black denote experimental averages.

Increasing the sprawl angle improves the accuracy of traversing along straight lines. Figure 5 indicates that after a 3.5 sec run time, the upright configuration results in an average leftward error of over 250 mm from the desired straight line path, while the sprawled configuration results in a mean error of under 50 mm. This significant increase in the path following error suggests that sprawling can have drastic positive effect on motion stability. Capturing the variability among paths is outside the focus of the present paper; this can be achieved by applying the Probabilistic Model Validation methodology reported in [18]. In another set of tests, it is verified that smaller sprawl angles allow tighter turns. To perform these turns during the experiments, the robot was set at 25% power on one side while the other side ran at full power.

Figure 6 suggests that the robot is capable of passively regulating its sprawl angle when following straight-line paths, and appears to converge to a steady-state height. This capability can contribute toward reducing the bouncing effect often observed in legged robots with spoked legs.

B. Passive lateral stability

From the upright configuration, PSR has the ability to passively change the sprawl angle on each of its two wheel-leg planes. Our tests confirm this capability by letting one side of the robot run over a 50 mm-tall obstacle, while the other side maintained contact with the flat ground surface, realizing the scenario depicted graphically in Fig. 7.

The height variation affects the roll angle of all articulated robot components: left-side spoked legs, body, and right-side spoked legs. The asymmetrical sprawl ability is evident in the different roll angle profiles shown for the articulated components mentioned above in Fig. 7. With the obstacle on the right hand side of the robot (see Fig. 7), the left pivot remains vertical with respect to the body, while the right side on top of the obstacle pivots. This behavior occurs when traversing elevated obstacles with the wheel-leg planes initially in an upright configuration. The reason is that once sprawling is initiated on the left side, the tipping moment is no longer present to pinch the left pivot against the body.

Decreased elevation has a similar effect as asymmetrical obstacles. An example is the robot dropping off from a surface. In the trials reported here, as PSR approaches a 5 cm drop off (Fig. 8) from a sprawled configuration, we observe a behavior similar to that shown in Fig. 7. With the drop on the left side of the robot, the right side pivots, allowing the left to drop down—thus reducing the roll of the body frame. Had the robot remained in the sprawled configuration during the drop, it would have either lost traction, or twisted about the roll-axis possibly causing a deviation from its forward trajectory. However, due to the passive compliance in the pivot joints, PSR was able to continue its forward motion with little impact on the shape of the resulting path.

C. Slope traversal

Moving on inclines of significant slope can be challenging for vehicles, and legged ones in particular due to the increased clearance they maintain with their supporting surface (cf. [19]). Existing work at the miniature scale utilizes adhesive contact [20]. Especially when the incline is uneven, the chance of flipping over can be significant, exacerbated by the bouncing and roll oscillation effects that occur at high

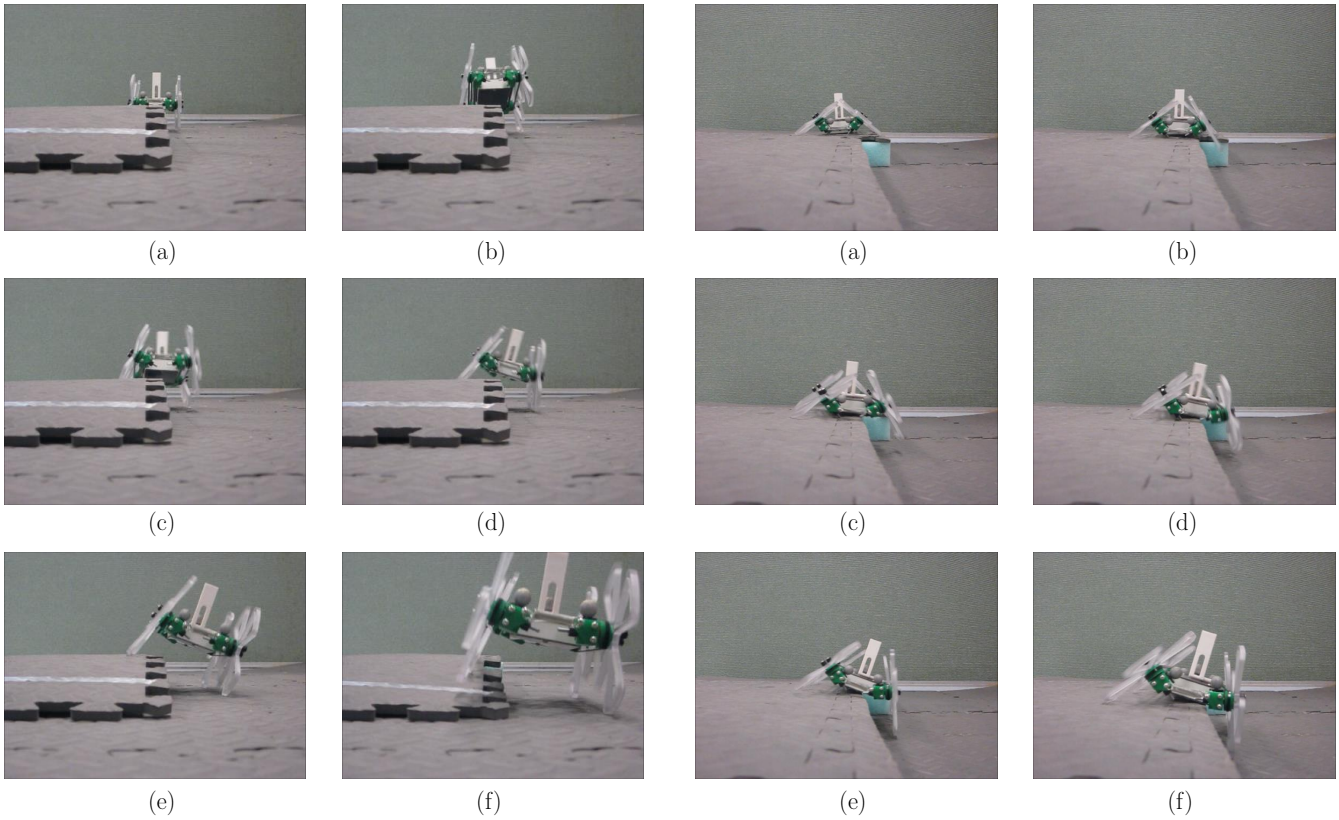

Fig. 7. Lateral stability when traversing uneven elevated terrain: (a) The robot in upright posture; (b) front wheel-legs lift off the ground as the obstacle is encountered; (c) right pivot begins to sprawl as the left side touches back the ground; (d) right side entirely on top of the obstacle and left entirely off; (e) sprawl of the left side as right side is pinched against the body of the robot; (f) the obstacle is cleared with minimal heading error.

Fig. 8. Lateral stability when traversing an uneven dropoff. (a) The robot in sprawled posture; (b) left front wheel-legs in mid-air above the drop off before moving downward; (c) just before the left rear whegs drop downward; (d) the right side sprawls as the left fully drops 5 cm; (e) the sprawl of the left side as the right side pinched against the body of the robot; (f) the left side pinched against the body as the robot progresses forward.

speed motion [9]. In our experimental tests, we observed that both ground clearance and bouncing are reduced with an increase in the sprawl angle. It is therefore expected that sprawling can have a beneficial effect on slope traversal.

Indeed, our tests on slope traversal at angles of 10, 20, and 30 degrees, validated our hypothesis that flip-on can be avoided with passive sprawling. However, the lack of adequate friction between the robot's spoked legs and the supporting surface was evident. Fig. 9 indicates that the robot is able to climb 10 and 20 degree slopes on a rubber floor mat with minimal slipping, but at a 30 degree angle there is not sufficient friction to propel the robot forward. In fact, even with continuous power to the motors with wheel-legs attempting to propel the robot up the slope, the robot still slid back down the rubber floor mat. We anticipate that adding rubber pads to the rounded plastic wheel-legs will increase friction and allow traversal of greater slopes.

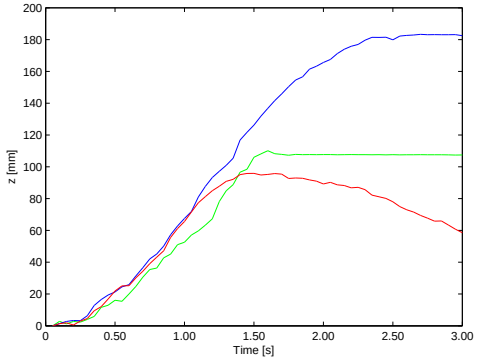

Fig. 9. The robot reaches the top of the 10 degree slope (in green) at the fastest rate; the 20 degree slope (in blue) and the 30 degree slope (in red) cannot be traversed for the given friction coefficients. In the latter case, the robot slides backward once the motors stop spinning.

D. Impact survivability

Rigid wheel-leg designs usually feature thin spokes (e.g., [3]). In the event of a fall from some height, the thin spokes are forced to absorb impact forces in their entity. The high magnitude impact forces occuring in accidental or deliberate falls increase the risk of spoked leg failure, due to the high stress concentrations along the thin spokes. Our tests verify that the passive sprawl capability can alleviate the effects of impact, by automatically directing the kinetic energy to the sprawl springs and absorbing the shock.

In our test, PSR is dropped from configurations at a height of *one meter*, with initial roll–pitch–yaw angles close to zero.[1] In all cases, the vehicle recovered from impact with no

[1]Obviously, dropping the robot on its side will not allow the sprawl mechanism to absorb any of the energy of the fall.

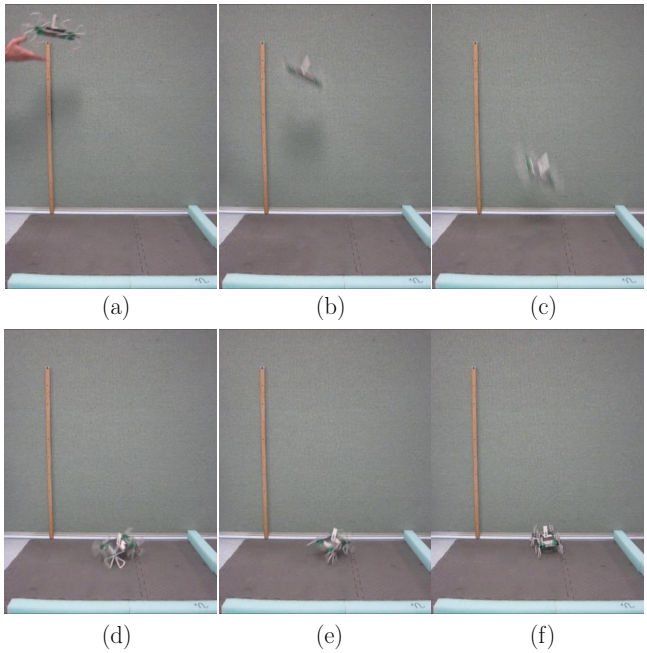

Fig. 10. (a) The robot is released from a height of one meter; (b)–(c) the robot as it falls freely without significant change in heading; (d)–(e) springs absorb the impact by allowing the robot to sprawl; (f) Sprawling effect causes some change in heading, but PSR stands with no structural damage.

structural damage. Although it is anticipated that increasing the height will eventually result in failure, these tests do confirm the robustness of the mechanism, and its potential for dynamic aerial deployment.

Snapshots in Fig. 10 show how the robot's compliant joints pivot under impact. Note that springs did not deform plastically in any of the trials, and thus impacts were safe and repeatable.

V. Conclusions

3D-printing has been proven to be an effective method for constructing legged robots at a miniature scale. Several successful existing designs utilize spoke-type legs and a recently developed robot [4] exhibits adjustable sprawling characteristics. This paper offers some first evidence that sprawling with passive compliance might be advantageous in terms of robustness to falls from moderate heights, improvement of lateral stability, and slope traversal. It is also demonstrated experimentally that although passive, the sprawl angle of the robot can be regulated by activating specific motion behaviors. Ongoing work investigates the suitability of bio-inspired kinematic [21], [22], and dynamic [14], [23], [24] models in capturing elementary motion behaviors of PSR.

References

[1] S. Kim, J. E. Clark, and M. R. Cutkosky, "iSprawl: Design and Tuning for High-speed Autonomous Open-loop Running," *The International Journal of Robotics Research*, vol. 25, no. 9, pp. 903 – 912, Sep. 2006.

[2] J. Morrey, B. Lambrecht, A. Horchler, R. Ritzmann, and R. Quinn, "Highly Mobile and Robust Small Quadruped Robots," in *IEEE/RSJ International Conference on Intelligent Robots and Systems*, vol. 1, 2003, pp. 82–87.

[3] B. Lambrecht, A. D. Horchler, and R. Quinn, "A small, insect-inspired robot that runs and jumps," in *IEEE International Conference on Robotics and Automation*, 2005, pp. 1240 – 1245.

[4] D. Zarrouk, A. Pullin, N. Kohut, and R. S. Fearing, "STAR - a sprawl tuned autonomous robot," in *IEEE International Conference on Robotics and Automation*, 2013, pp. 20 – 25.

[5] C. Brown, D. Vogtmann, and S. Bergbreiter, "Efficiency and effectiveness analysis of a new direct drive miniature quadruped robot," in *IEEE International Conference on Robotics and Automation*, 2013, pp. 5631–5637.

[6] R. Wood, S. Avadhanula, R. Sahai, E. Steltz, and R. S. Fearing, "Microrobot Design Using Fiber Reinforced Composites," *Journal of Mechanical Design*, vol. 130, no. 5, pp. 1 – 11, May 2008.

[7] A. M. Hoover, S. Burden, X.-Y. Fu, S. Sastry, and R. S. Fearing, "Bio-inspired design and dynamic maneuverability of a minimally actuated six-legged robot," in *IEEE International Conference on Biomedical Robotics and Biomechatronics*, 2010, pp. 869–876.

[8] A. Pullin, N. Kohut, D. Zarrouk, and R. S. Fearing, "Dynamic turning of 13 cm robot comparing tail and differential drive," in *IEEE International Conference on Robotics and Automation*, 2012, pp. 5086–5093.

[9] D. Haldane, K. Peterson, F. Garcia Bermudez, and R. S. Fearing, "Animal-inspired design and aerodynamic stabilization of a hexapedal millirobot," in *IEEE International Conference on Robotics and Automation*, 2013, pp. 3279 – 3286.

[10] R. Fearing, "Challenges for Effective Millirobots," in *IEEE International Symposium on Micro-NanoMechatronics and Human Science*, 2006.

[11] R. Altendorfer, N. Moore, H. Komsuoglu, H. Brown Jr., D. McMordie, U. Saranli, R. Full, and D. E. Koditschek, "RHex: A biologically inspired hexapod runner," *Autonomous Robots*, vol. 11, pp. 207–213, 2001.

[12] M. Klein, A. Boxerbaum, R. Quinn, R. Harkins, and R. Vaidyanathan, "SeaDog: A rugged mobile robot for surf-zone applications," in *4th IEEE RAS & EMBS Int. Conf. on Biomedical Robotics and Biomechatronics*, 2012, pp. 2155 – 1774.

[13] H. Komsuoglu, K. Sohn, R. Full, and D. Koditschek, "A physical model for dynamical arthropod running on level ground," in *International Symposium on Experimental Robotics*, 2008.

[14] P. Holmes, R. J. Full, D. E. Koditschek, and J. Guckenheimer, "The Dynamics of Legged Locomotion: Models, Analyses, and Challenges," *SIAM Review*, vol. 48, no. 2, pp. 207–304, 2006.

[15] K. Meijer, T. Libby, and R. Full, "Passive stability provided by the musculo-skeletal properties of an insect leg," *American Zoologist*, vol. 40, no. 6, pp. 1129–1130, 2000.

[16] K. Karydis, D. Zarrouk, I. Poulakakis, R. S. Fearing, and H. G. Tanner, "Planning with the STAR(s)," in *IEEE/RSJ International Conference on Intelligent Robots and Systems*, 2014, pp. 3033–3038.

[17] A. Boxerbaum, J. Oro, and R. D. Quinn, "Introducing dagsi whegs: The latest generation of whegs robots, featuring a passive-compliant body joint," in *IEEE International Conference on Robotics and Automation*, 2008.

[18] K. Karydis, I. Poulakakis, and H. G. Tanner, "Probabilistic validation of a stochastic kinematic model for an eight-legged robot," in *IEEE International Conference on Robotics and Automation*, 2013, pp. 2562 – 2567.

[19] M. Raibert, K. Blankespoor, G. Nelson, and R. Playter, "BigDog, the rough-terrain quadruped robot," in *17th IFAC World Congress*, 2008, pp. 10 822 –10 825.

[20] K. Daltorio, A. Horchler, S. Gorb, R. Ritzmann, and R. Quinn, "A small wall-walking robot with compliant, adhesive feet," in *IEEE/RSJ International Conference on Intelligent Robots and Systems*, 2005, pp. 3648–3653.

[21] K. Karydis, I. Poulakakis, and H. G. Tanner, "A switching kinematic model for an octapedal robot," in *IEEE/RSJ International Conference on Intelligent Robots and Systems*, 2012, pp. 507–512.

[22] K. Karydis, Y. Liu, I. Poulakakis, and H. G. Tanner, "A Template Candidate for Miniature Legged Robots in Quasi-Static Motion," *Autonomous Robots*, 2014, in print.

[23] J. Schmitt and P. Holmes, "Mechanical models for insect locomotion: dynamics and stability in the horizontal plane I. Theory," *Biological Cybernetics*, vol. 83, no. 6, pp. 501–515, Nov. 2000.

[24] ——, "Mechanical models for insect locomotion: dynamics and stability in the horizontal plane - II. Application," *Biological Cybernetics*, vol. 83, no. 6, pp. 517–527, Nov. 2000.